

Supplementary material:

Ligand-dependent nano-mechanical properties of CdSe nanoplatelets: calibrating nanobalances for ligands affinity monitoring.

Quentin Martinet¹, Justine Baronnier¹, Adrien Girard², Tristan Albaret¹, Lucien Saviot³, Alain Mermet¹, Benjamin Abecassis⁴, Jérémie Margueritat^{1} and Benoît Mahler^{1*}.*

¹Institut Lumière Matière Université de Lyon, Université Claude Bernard Lyon 1, UMR CNRS 5306, F-69622 Villeurbanne, France

²Sorbonne Université, CNRS UMR8233, MONARIS, Paris, France

³Laboratoire Interdisciplinaire Carnot de Bourgogne UMR 6303 CNRS-Université de Bourgogne Franche-Comté, 9 avenue A. Savary, BP 47870, 21078 Dijon Cedex, France

⁴Univ Lyon, ENS de Lyon, CNRS, Université Claude Bernard Lyon1, Laboratoire de Chimie UMR 5182, F-69342 Lyon, France

A. Effect of the surface concentration at the surface of a Nanoplatelet

The surface concentration used in the paper was deduced by considering that a ligand can bind with 2 Cd⁺ ions per unit cell of area a^2 , with $a = 0.608$ nm is the lattice parameter of CdSe zinc blende. Complete coverage (all Cd atoms on the surface are linked by a ligand) therefore corresponds to a surface concentration of 5.4 ligands.nm⁻². This assumption is probably an overestimation of the reality and figure S1 shows the effect of decreasing the surface concentration at 4.3 ligands.nm⁻² (80% of the Cd atoms are bond with a ligand). As the surface coverage decreases the theoretical frequency of the NPL vibration increases. The difference between experiment and theory therefore increases when the surface concentration is reduced and tends towards a constant frequency (free NPL vibration).

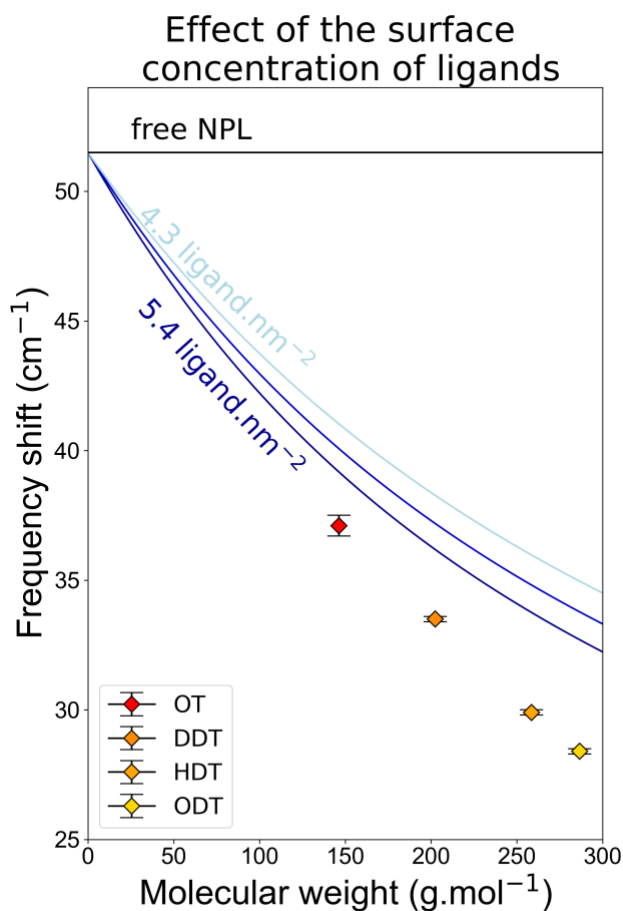


Figure S1: Effect of the surface density of ligand. The surface density was varied from 5.4 to 4.3 ligand.nm⁻² and injected into the massload model considering a 4 monolayers thick NPL. The upper horizontal line corresponds to a free NPL, that is to say a surface concentration of 0 ligand.nm⁻². Experimental data are also represented for comparison.

B. Effect of Cu doping

To resolve the Raman peaks, it is necessary to quench the luminescence of NPLs. To achieve this goal, we developed a copper doping technique to significantly reduce the luminescence yield. The raw Raman spectra of the doped and undoped NPLs of 4MLs are shown in figure S2. Both

spectra have been normalized to the intensity of the anti-stokes longitudinal optic mode peak for ease of comparison. When the doping ratio increases to 1Cu atom for 1000 Cd atoms, the luminescence background is drastically reduced, allowing Raman peaks to be resolved. On the blue curve, well-defined Raman peaks are observed at the same frequency than for the black curve, showing that the copper doping used (1/1000) has no effect on the vibrational properties of the NPLs.

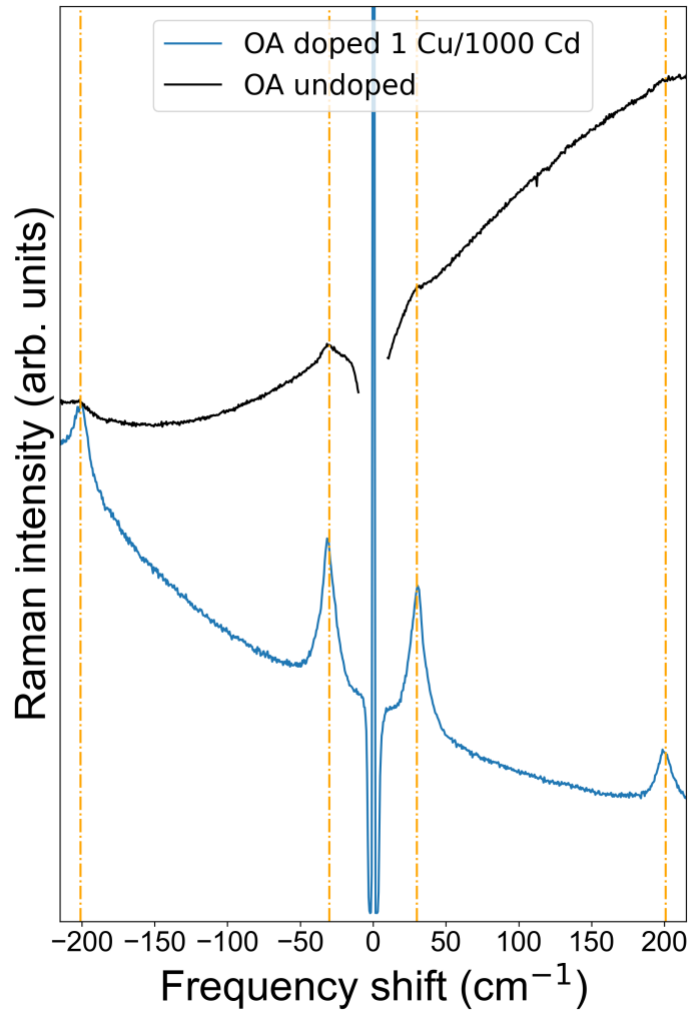
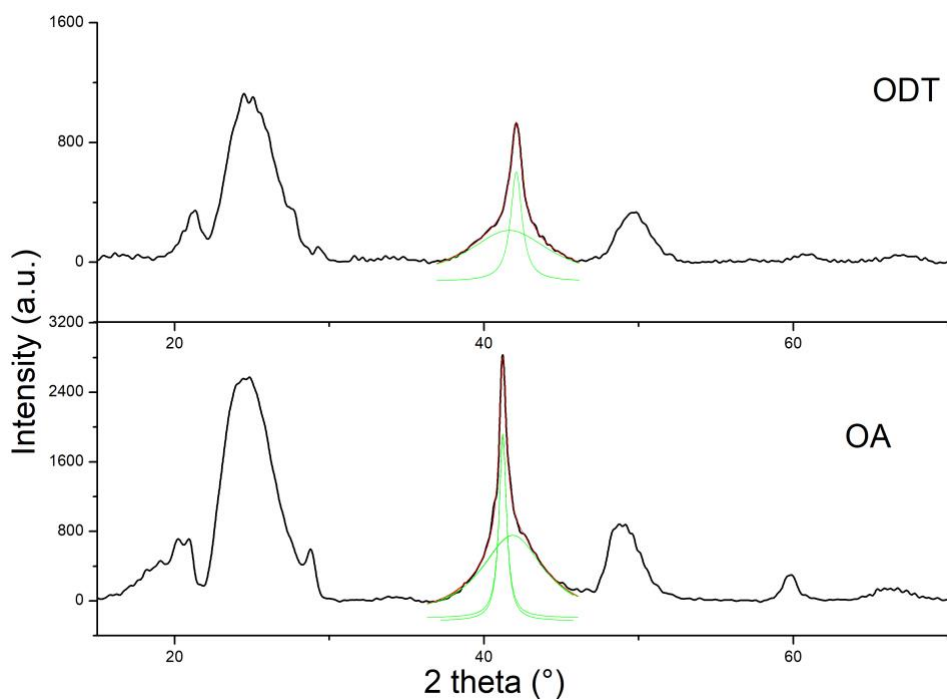


Figure S2: Raman spectra of NPLs of 4 MLs (510 nm exciton) with OA ligands. The black and blue curves correspond respectively to the Raman spectra of the undoped and doped (1Cu/1000Cd) NPLs. Vertical orange dotted lines are guides to the eyes. The spectra have been normalized to the intensity of the anti-Stokes LO phonons for a clear comparison.

C. Diffractograms



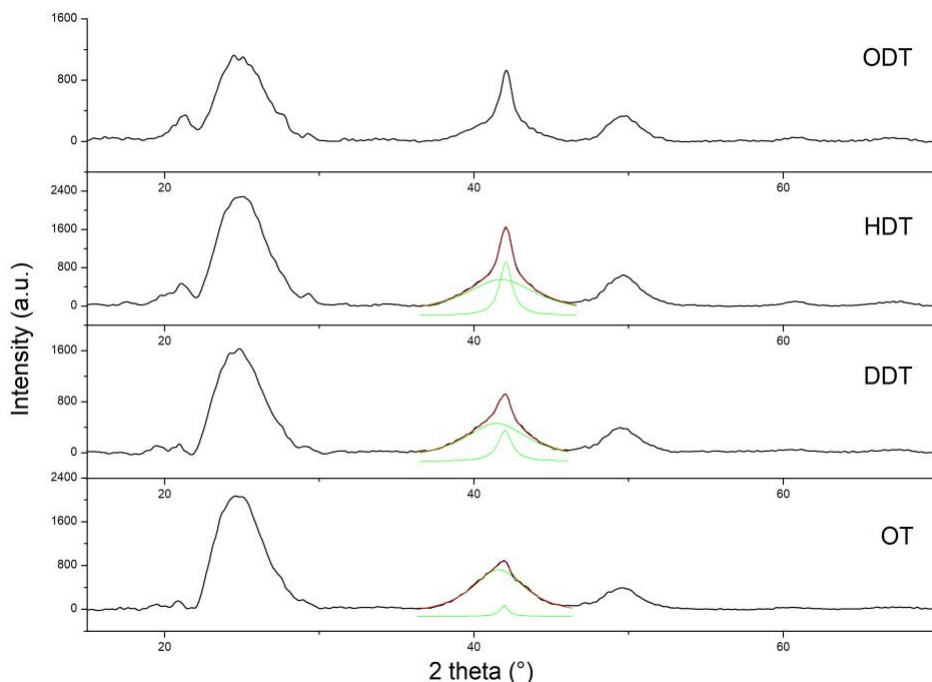


Figure S3: diffractograms and the associated fits to extract lattice parameters corresponding to 3ML CdSe NPLs from the same batch and different surface ligands: Oleic Acid (OA), Octadecanethiol (ODT), Hexadecanethiol (HDT) Dodecanethiol (DDT) and Octanethiol (OT).

D. Determining the effect of a lattice parameter variation on the elastic constant of bulk CdSe

The initial hypotheses are the following:

The crystalline structure is Zinc-Blende with $a_0 = 6.09500$ angstrom (after optimization). There are 8 atoms per cell (4 Cd, 4Se). Using these parameters, the elastic constant at 0K have been calculated by finite differences and are reported in table 1.

	C_{11}	C_{12}	C_{44}
CdSe (Zinc-Blende)	63.67 (± 0.02)	45.15 (± 0.01)	22.31 (± 0.002)

Table 1. Elastic constants (GPa) for zinc-blende CdSe at 0K calculated using VASP PBESOL

Using these values, we obtained a bulk modulus of 51.32 GPa.

We have then varied the lattice parameter along the crystalline direction a in the range -3 to +3 %. The lattice parameter along b and c are fixed to 6.0950 angstroms. We consider that C_{11} is the elastic modulus in the direction of the deformation, and C_{33} is the average along the two other directions (that must be equivalent). The obtained data are represented in figure S1.

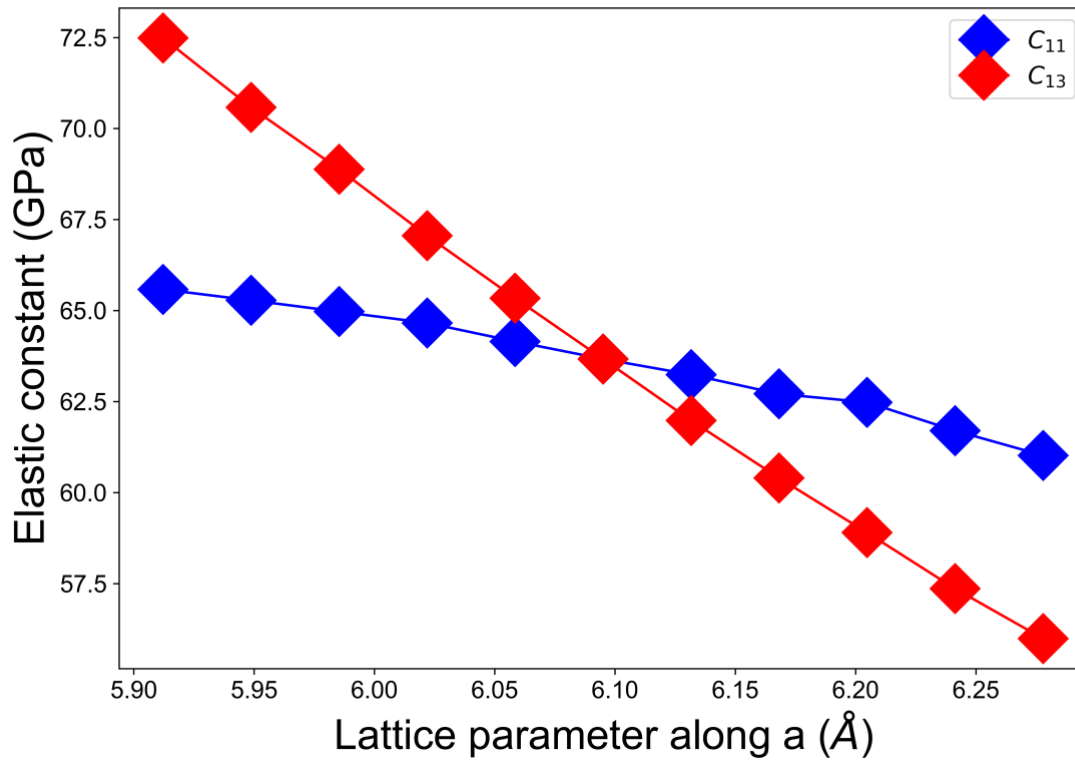


Figure S4. Dependency of the elastic constant C_{11} and C_{33} when the lattice parameter is modified along the crystalline direction a .

E. Experimental dependency of C_{33} parameter for 5 (4+1) and 6 (5+1) MLs.

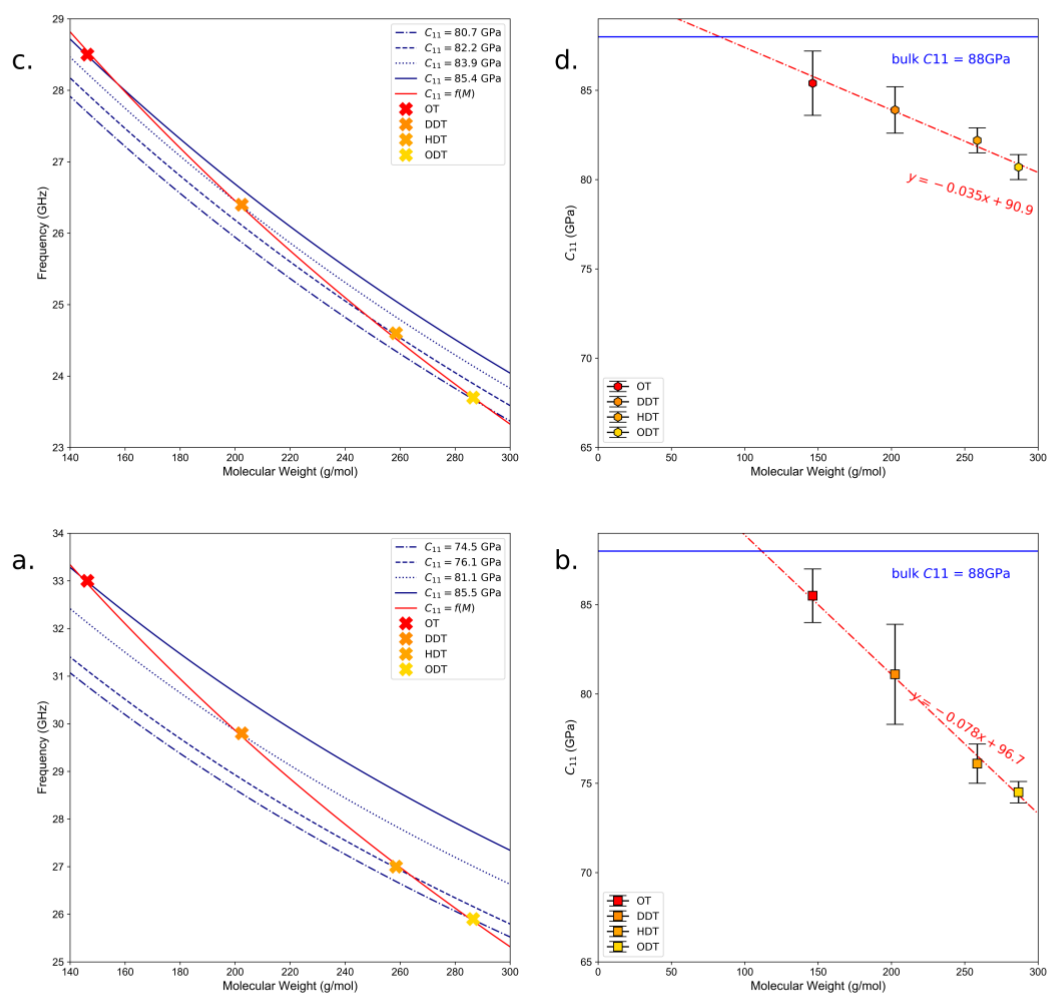


Figure S5. a. and c. fitting method: the blue lines correspond to the fit applying the mass-load model with a constant $C_{11}=C_{33}$ in the case of NPLs containing 5 (4+1) and 6 (5+1) MLs respectively. The crosses represent the measured frequencies. The red curve is the mass-load model considering the dependency of the C_{33} deduced from **b. and d.** which represents C_{33} as a function of the molecular weight for NPLs of 5 (4+1) and 6(5+1) MLs, respectively.

Figure S3 shows the fitting method applied to deduce the dependency of C_{33} as a function of the molecular weight. Typically, the C_{33} is considered as a free parameter in the mass-load model. Then a least square method is applied to compare the frequency measured and the calculated frequency at the same molecular weight (fixed parameter). The error bars in figure S2 b and d are calculated by considering the error deduced from the measurements. Finally, a linear fit is applied to deduce the elastic constant C_{33} dependency as a function of the molecular weight.